

Application of Woodward-Hoffmann ideas to solid-state polymorphic phase transitions with specific reference to polymerization of S_2N_2 and the black phosphorus to $A7$ (arsenic) structural transformation

Jeremy K. Burdett and Sarah L. Price*

Department of Chemistry, The University of Chicago, Chicago, Illinois 60637

(Received 28 September 1981)

The analog of the Woodward-Hoffmann orbital correlation diagrams for solid-state polymorphic phase transitions are defined (within the tight-binding approximation) and the implications of the form of the correlation diagram $E(\vec{k}, q)$ for the reaction kinetics are discussed. It is proposed that if an occupied orbital of the parent structure is transformed into an unoccupied orbital of the new structure at a point in \vec{k} space, then the reaction cannot proceed with retention of translation symmetry in the intermediate, and so can only proceed via a "nucleation-and-growth"-type mechanism. On the other hand, if the $E(\vec{k}, q)$ surface shows a smooth correlation of occupied levels of the reactants and products the process may proceed "martensitically." Correlation diagrams $E(\vec{k}, q)$ are constructed with the use of group-theoretical analysis and extended-Hückel band-structure calculations, and discussed for the following transformations: sodium chloride from the rocksalt to cesium chloride structure, the bond breaking and reforming in a linear chain of diatomic molecules, an idealized model of the polymerization of S_2N_2 to both the *cis* and *trans* polymers $(SN)_x$, and the transformation of black phosphorus into the $A7$ arsenic-type structure.

I. INTRODUCTION: WOODWARD-HOFFMANN IDEAS

Woodward and Hoffmann^{1,2} made an important advance in our understanding of organic reactions and our ability to design reactions to give the desired products by using the principle of the conservation of orbital symmetry to predict whether the symmetry of the occupied and unoccupied orbitals of the reactant and product would allow the reaction to proceed thermally or photochemically. Figure 1(a) shows an orbital correlation diagram, where the highest occupied molecular orbital (HOMO) of the reactant of a_1 symmetry becomes a high-energy unoccupied molecular orbital of the product. Hence an unoccupied reactant orbital of different symmetry (b_2) must correlate with an occupied orbital of the product. The crossing of the two orbitals of a_1 and b_2 symmetry at the point q_c along the reaction coordinate q implies that the energy of the electronic ground state goes through a maximum at q_c [Fig. 1(b)]. Since the HOMO and LUMO (lowest unoccupied MO) are usually separated by a significant energy gap in stable molecules, this high symmetry-imposed reaction barrier makes it unlikely for the reaction to proceed thermally (i.e., the crossing implies the reaction is "thermally forbidden"). However, if an electron is promoted from the a_1 to the unoccupied b_2 orbital (usually by irradiation with visible or ultraviolet light), for both the possible singlet and triplet states, the energy changes along q are very small and the reaction is thus "photochemically allowed."

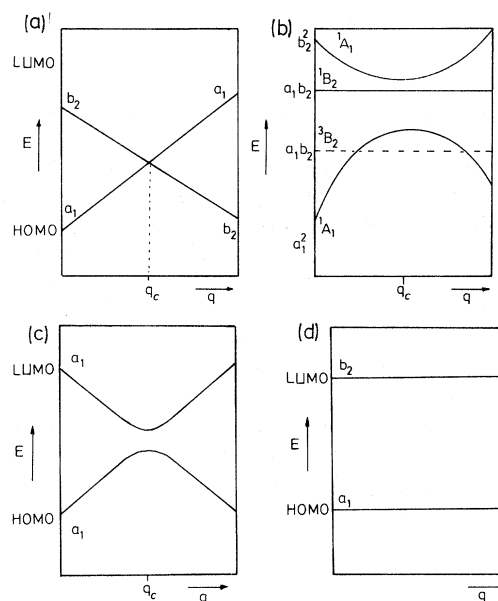


FIG. 1. Illustration of the Woodward-Hoffmann approach to molecular organic reactions. (a) Crossing of the highest occupied molecular orbital (HOMO) and the lowest unoccupied molecular orbital (LUMO), which have different symmetry (a_1 and b_2 chosen for illustration) along a reaction coordinate q . (b) The state correlation diagram corresponding to the orbital correlation diagram shown in (a). (c) An avoided crossing of two molecular orbitals which will give rise to a state energy diagram similar to that in (b). (d) A different orbital correlation diagram where there is no HOMO-LUMO crossing. Here the state correlation diagram will look similar to the orbital correlation diagram and there is no symmetry-imposed reaction barrier.

Such molecular orbital correlation diagrams can be simply constructed when the reaction intermediate has some symmetry element which constrains the form of the orbitals which are changing during the reaction (e.g., a mirror plane through a bond which is being made or broken). However, the great utility of the Woodward-Hoffmann ideas for organic reactions in general arises because the results from the analysis of a high-symmetry reaction also apply to related, less symmetrical systems, where, for example, there are different substituents attached to the "reacting part" of the molecule. Figure 1(c) shows such a case, where the reaction intermediate has approximately the same geometry but lower point symmetry than the intermediate in Fig. 1(a). Here the HOMO and LUMO are technically of the same symmetry. Mixing between these two orbitals is small in the case shown here and an avoided crossing occurs at q_c . The state correlation diagram, however, will be similar to that of Fig. 1(b) and this reaction is again thermally forbidden but photochemically allowed.

The other type of orbital correlation diagram is shown in Fig. 1(d), where there is smooth correlation between the occupied orbitals of the reactants and products. Clearly the corresponding state correlation diagram will not have a symmetry-imposed barrier to the reaction, and the transformation is thermally allowed.

However, even if a reaction is allowed by orbital symmetry considerations this is no firm guarantee that the reaction will actually occur. The Woodward-Hoffmann ideas are solely concerned with the symmetry-controlled kinetics of the reaction; there may be a substantial energy barrier to reaction with other origins, or the process may simply be thermodynamically unfavorable. Note that the Woodward-Hoffmann diagram considers a concerted reaction along a particular reaction pathway. Other pathways may be possible, and in molecular organic chemistry there is often an alternative radical reaction route (which is not a concerted process and so cannot be tackled using the Woodward-Hoffmann approach) which can lead to the formation of supposedly "forbidden" products.

There have been only a few, very specific attempts³ to apply the Woodward-Hoffmann approach to solid-state reactions (the solid-state analogy to molecular reactions are more usually termed polymorphic phase transitions). This is due in part to the fact that, whereas the molecular orbitals of organic molecules are small in number, and can be readily derived using the (often high) symmetry of the molecule, the orbitals of solid-state "infinite molecules" are defined in terms of the Bloch functions which take into account the translational symmetry, and are usually represented by the electronic band structure of the solid.

This work discusses the application of the basic Woodward-Hoffmann principles to solid-state reac-

tions. The methodology and the conclusions are somewhat altered by the infinite nature of the solid. We also present some of the first studies relating the band structure of the reactant and product of some model and real solid-state structural changes, emphasizing the symmetry aspects of the reactions.

II. THEORY

Let us begin, for the sake of the argument, with the assumption that translational symmetry is preserved during solid-state transformations between structurally related polymorphs, i.e., the atomic movements in the different unit cells are "in phase" or "cooperative." This is the solid-state equivalent of the "concerted" process noted above. In such cases, we may generalize the Woodward-Hoffmann diagram to a five-dimensional plot $E(\vec{k}, q)$, illustrating how the energy of each orbital at every point in \vec{k} space (3 coordinates) varies with the reaction coordinate q . During a transformation, the shape of the unit cell will often change, however, the \vec{k} vectors will always be defined by the \vec{k} vector basis of the unit cell at the point in the reaction.

Three types of $E(\vec{k}, q)$ surface can be conceived.

(a) All the occupied molecular orbitals of the reactant correlate smoothly, with q , to the occupied molecular orbitals of the product at every point in \vec{k} space. Such a reaction would, by analogy with the Woodward-Hoffmann rules, be "thermally allowed" (in the solid state this would include reactions which occur on the application of pressure and shear stress, as well as heating), and so may proceed with the retention of translational symmetry during the course of the reaction. We might expect this type of $E(\vec{k}, q)$ surface to be very common, as it would describe some high- and all low-symmetry transformations, since when all the orbitals have the same nontranslational symmetry they can "mix" during the distortion (for all \vec{k}), thus avoiding any crossings. (However, for low-symmetry transformations there may still be avoided crossings on $E(\vec{k}, q)$ [cf. Fig. 1(c)].)

(b) An occupied orbital of the reactant correlates with an unoccupied orbital of the product at every point in \vec{k} space. This is the analogy to the Woodward-Hoffmann diagram for "thermally forbidden" reactions. However, this requires the intersection of two orbital surfaces $E^{\text{occ}}(\vec{k}, q)$ and $E^{\text{unocc}}(\vec{k}, q)$, implying that for every \vec{k} there must be some value of q at which the two orbitals cross. This behavior is physically impossible, because at low-symmetry \vec{k} vectors, the two orbitals would have the same symmetry, and by mixing would avoid such a crossing.

(c) The occupied orbitals of the reactant and product correlate smoothly with q at low-symmetry \vec{k} vectors, but at certain high-symmetry \vec{k} vectors and

OMO and UMO have different symmetry, and so can cross at some point along the reaction coordinate. For \vec{k} vectors of lower symmetry, but close in \vec{k} space to vectors of high symmetry where there is an OMO-UMO crossing, the correlation diagram would show a narrowly avoided crossing similar to that in Fig. 1(c).

It is the possibility of this third type of behavior in transformations between structurally related solids which is novel and of particular interest. The existence of crossings on the $E(\vec{k}, q)$ surface (c) implies that the reaction path, which by assumption maintains the translational symmetry during the reaction, is unfavorable. This electronic reaction barrier could be removed if the reaction were to proceed by a noncooperative mechanism, such that, during the course of the reaction, the moving atoms were in a region where the short-range translational symmetry had been destroyed. Naturally such a reaction mechanism could not be described by an $E(\vec{k}, q)$ surface, as the destruction of the translational symmetry invalidates the symmetry label \vec{k} . (The organic molecular analogy might be the radical pathway for reaction.)

One of the attractions of the Woodward-Hoffmann analysis of chemical reactions is that it is not generally necessary to calculate the energies of the orbitals, as the existence or not of an OMO-UMO crossing can often be derived from symmetry arguments. In determining the existence of crossings on an $E(\vec{k}, q)$ surface, it would be tedious and unnecessary to map out the whole surface. Standard group theoretical techniques and tables can be used to predict the possible symmetry species of the orbitals at various points in \vec{k} space, and it is only at certain high-symmetry \vec{k} points and directions that the group of the wave vector contains sufficient symmetry elements for crossings to be possible. Also, from a simple viewpoint, we note that the orbitals which will vary most in energy during a reaction, will be those whose \vec{k} vectors have significant components in the direction in which there is significant rearrangement of the atoms. Hence, if there are any OMO-UMO crossings on the $E(\vec{k}, q)$ surface, they will probably occur at high-symmetry \vec{k} vectors, where the \vec{k} -vector direction is related to the distortion coordinate. Hence we can determine the existence of OMO-UMO crossings without the major task of analyzing sufficient \vec{k} points to represent the entire $E(\vec{k}, q)$ surface. We shall describe some examples later in this paper.

III. RELATIONSHIP BETWEEN $E(\vec{k}, q)$ SURFACES AND EXPERIMENTAL SOLID-STATE REACTION TYPES

The conclusion drawn above, that the nature of the $E(\vec{k}, q)$ surface for a specific solid-state polymorphic

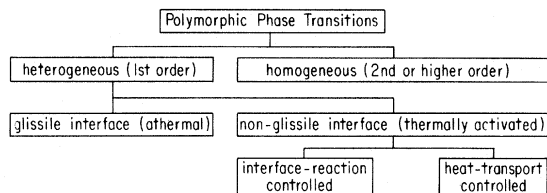


FIG. 2. Modified version of Christian's classification scheme for phase transformations in solids based on growth processes. This version is appropriate for polymorphic phase transitions.

transformation determines whether it is possible or impossible for the transformation to proceed with approximate retention of translational symmetry, is only useful if it can be related to the experimentally observed properties of such reactions.

There are several different classifications⁴ of composition-invariant, solid-state phase transitions, but the most useful for this present discussion is that developed by Christian,⁵ based on the experimentally observable nature of the growth process of the product structure within the parent structure. The relevant part of this classification scheme is shown in Fig. 2.

A. Homogeneous reactions

Homogeneous reactions are those in which the product phase begins to form simultaneously everywhere within the parent and a diffuse interface exists between the two phases. This type of reaction behavior would almost certainly involve the approximate retention of translational symmetry during the course of the reaction. However, such reactions correspond to second, or higher-order, thermodynamics, and hence invariably involve only small displacements of the atoms. Although many reactions of this type are interesting, such as $\alpha \rightleftharpoons \beta$ quartz and certain ferroelectric transitions, the transformation paths are such that we would not expect sufficient change in the HOMO and LUMO energy levels during the transformation for a crossing to be possible. We expect surface type (a) behavior and although the course of such reactions are consistent with the theory, they are not likely to provide any really useful applications or tests of the ideas developed here.

B. Heterogeneous reactions

Heterogeneous reactions are defined⁵ as those where, at an intermediate stage, the assembly can be divided into macroscopically distinct regions, some of which have transformed and the rest have not. These transformations are thermodynamically first order, and the product forms a discrete nuclei. These

transformations are subdivided into two groups; nucleation and growth, where the interface is nonglissile (i.e., requires a large activation energy for movement), and martensitic reactions, named after the polytypic reaction in steels, where the interface is glissile, and in some cases moving with extreme rapidity, even on a macroscopic scale. However, many reactions of an intermediate character have been recognized, and some reactions may occur by either type of mechanism, depending on the conditions.

During the course of a nucleation and growth transformation, the symmetry around a moving atom at the interface between the parent and product phases is low. Thus, as far as the term "nucleation and growth" implies the loss of local translational symmetry during the reaction, it is the classification for all reactions which would involve an OMO-UMO crossing on the $E(\vec{k}, q)$ surface.

Martensitic reactions⁵ utilize the cooperative movements of many atoms, and since most atoms have the same nearest neighbors (differently arranged) in the two phases, the net movements are such that, in a small enough region, a set of unit cells of the original phase is effectively homogeneously deformed into a corresponding set of cells of the new phase, and hence the translational symmetry is approximately retained during the reaction. Discrete regions of the solid usually transform suddenly, often with a very high velocity which is almost independent of temperature, and since there is generally a change in the shape of the unit cell during the transformation, an observable shape change on an originally flat polished surface is often developed. The definition of a martensitic reaction is often related to such an experimentally observed shape change, whereas, for the purpose of our thesis, the crucial characteristic is the approximate retention of translation symmetry during the course of the reaction.

With the above distinction in mind, our thesis is that reactions which have an $E(\vec{k}, q)$ with no OMO-UMO crossings may proceed martensitically, whereas, if there are such crossings on the $E(\vec{k}, q)$ surface, the reaction cannot proceed martensitically, but will have to proceed via nucleation and growth. In the rest of this paper we test out this hypothesis for some solid-state transformations, first for an ionic system, and then for covalently bonded systems starting with some examples of pedagogical interest.

IV. APPLICATIONS AND RESULTS: CALCULATION OF $E(\vec{k}, q)$ SURFACES FOR THE TRANSFORMATION FROM THE ROCKSALT TO CESIUM CHLORIDE STRUCTURE

Many alkali halides which normally have the rocksalt structure adopt the cesium chloride structure at

high pressure. Conversely cesium chloride and some ammonium halides change to the rocksalt structure at high temperatures.⁶ This transformation was modeled (for NaCl) with a body-centered rhombohedral unit cell as the reaction intermediate. The rocksalt structure ($q = 0$) corresponds to a rhombohedral angle $\theta = 60^\circ$, and the cesium chloride structure ($q = 1$) to $\theta = 90^\circ$ (Fig. 3). The transformation consisted of increasing θ and adjusting the length of the side of the rhombohedron such that the shortest Na-Cl distance remained constant at the experimental value of 2.814 Å. (In the systems which undergo this transformation,⁶ the shortest $A-B$ distance usually alters by only a few percent between the two structures; and some assumption of this nature has to be made in order to define a model for the transformation.)

As for all our examples, the electronic band structure for the valence orbitals was calculated using the extended Hückel method⁷ with parameters given in the Appendix. Because of the crude nature of such calculations, the numerical values for the energy changes are expected to be very approximate, however, the general form of the $E(\vec{k}, q)$ surface, and the existence or absence of crossings (which will be predominantly determined by symmetry), is expected to be reliable.

From calculations at $\theta = 60^\circ$, 75° , and 90° at various \vec{k} values (defined relative to the rhombohedral cell at the appropriate θ), it is clear that the occupied levels of NaCl in the rocksalt structure transform in a smooth and logical manner to those of the cesium chloride structure (Fig. 4), giving rise to an $E(\vec{k}, q)$ surface of type (a). Indeed, this could be predicted, since the occupied orbitals are dominated by the chlorine s and p atomic orbitals for both structures. For this reason, all $E(\vec{k}, q)$ surfaces for transformations between very ionic octet systems will be of class (a), and hence, it is predicted, could proceed "martensitically." Ammonium bromide has been observed to undergo this transformation martensitically⁸ under certain conditions thus supporting this conclusion.

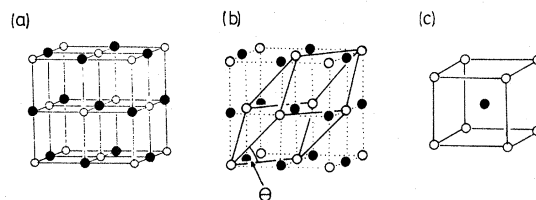


FIG. 3. Reaction coordinate for the rocksalt to cesium chloride structural transformation. (a) Conventional unit cell for the rocksalt structure. (b) Rhombohedral unit cell for the rocksalt structure. On increasing the rhombohedral angle from 60° to 90° , this becomes the unit cell of the cesium chloride structure shown in (c).

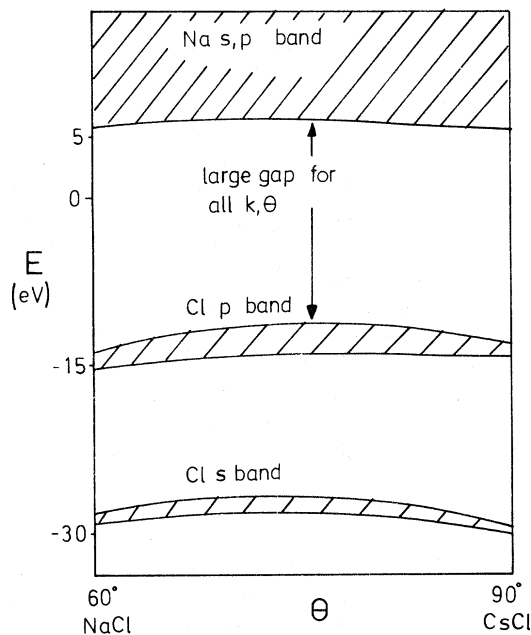


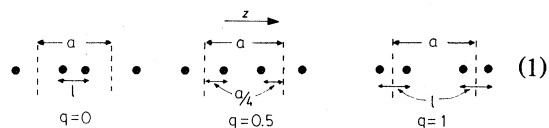
FIG. 4. Slices through schematic $E(\vec{k}, q)$ surfaces for the rocksalt to CsCl structural transformation (θ is defined in Fig. 3).

We now turn our attention to the possibility of HOMO-LUMO crossings on $E(\vec{k}, q)$ surfaces for transformations between covalently bonded structures.

V. LINEAR CHAIN

One particularly simple example, which illustrates how HOMO-LUMO crossings arise when the prob-

lem contains translational symmetry, is the theory associated with the transformation shown in diagram (1).



Here the linkages between initially bonded pairs of atoms are severed as the atoms move apart, and bonds form between the initially nonbonded adjacent atoms. At the midpoint in the transformation ($q = 0.5$), each atom is symmetrically situated a distance $a/2$ from both of its neighbors, where a is the unit-cell length. Figure 5 shows the energy levels E_i (within the tight-binding approximation) and their variation with \vec{k} and $q[E_i(\vec{k}, q)]$ for the hypothetical one-dimensional infinite chain of P_2^{4-} , which is isoelectronic with Cl_2 . This diagram can be understood by noting that the orbitals at $\Gamma(k_z = 0)$ are similar in character and energy to those of the isolated P_2^{4-} molecule, i.e., two pairs of σ bonding and antibonding orbitals (σ_g^+ , σ_u^+) derived from the $3s$ and $3p_z$ atomic orbitals, and a π bonding (π_u) and antibonding (π_g) pair derived from the $3p_{x,y}$ atomic orbitals [Fig. 5(a)]. The actual form of the diagrams will depend on the extent of $s-p$ mixing and the order of the $2\sigma_g$ and $1\pi_u$ orbitals is often reversed.⁹ However, the important features of the diagram derive from symmetry aspects of this system.

The most notable features of the $E(\vec{k}, q)$ surface is the sticking together of all the pairs of orbitals at $k_z = \frac{1}{2}$, $q = 0.5$. This can be understood in terms of Herring's theorem^{10,11} as a result of either the extra symmetry of the system at $q = 0.5$, or equivalently

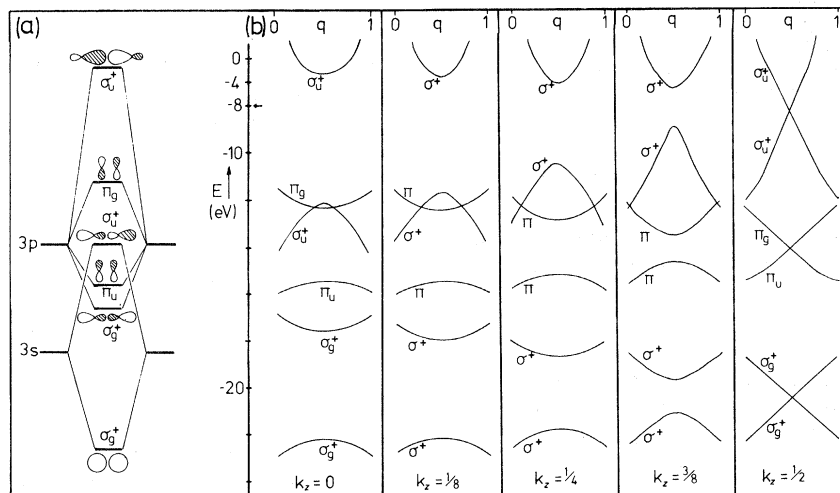


FIG. 5. (a) The derivation of the energy levels of a P_2^{4-} molecule, which corresponds to the orbitals of the infinite chain of P_2^{4-} at $k_z = 0$. (b) Slices through the $E(\vec{k}, q)$ surfaces for the linear transformation shown in diagram (1). (Note the scale change indicated by the arrow.)

because a smaller unit cell could be defined at this point in the transformation. As can be seen from the last ($k_z = \frac{1}{2}$) diagram of Fig. 5, this symmetry-imposed degeneracy is the crossing point for all the pairs of orbitals.

It is interesting to investigate the electronic reasons behind these crossings occurring at $k_z = \frac{1}{2}$, and not at $\Gamma(k_z = 0)$. This occurs because the orbitals of one unit cell are exactly in phase with the orbitals in the adjacent unit cells at $k_z = 0$, but at $k_z = \frac{1}{2}$, they are exactly out of phase. Figure 6 shows how the π_u and π_g orbitals remain bonding and antibonding, respectively, throughout the transformation at $k_z = 0$, but at $k_z = \frac{1}{2}$, the orbitals have equal energy at $q = 0.5$ as a direct result of the equality of intracell and intercell interactions. As q increases further the π_u orbital becomes increasingly antibonding and the π_g increasingly bonding. Note that the crossing occurs as a result of the translational symmetry; the π_u and π_g orbitals remain bonding and antibonding, respectively, between the two atoms within the unit cell chosen initially.

The effect of these orbital crossings on the energet-

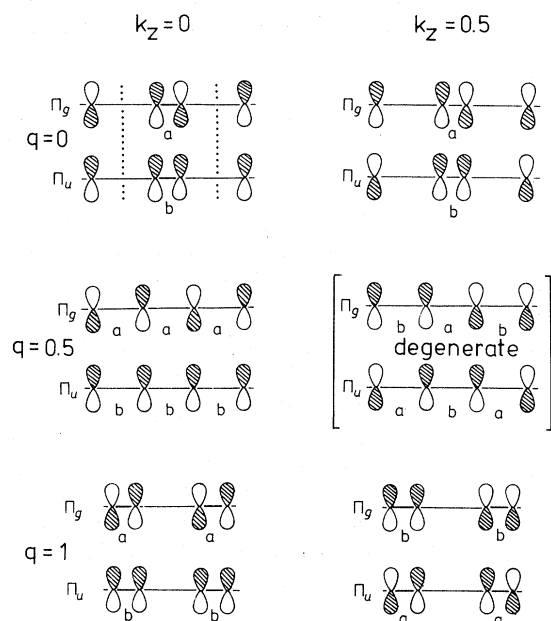


FIG. 6. Orbital changes during the breaking and reformation of bonds within a linear chain of P_2^{4-} molecules. At $k_z = 0$, a bonding orbital remains bonding during the bond reformation process, but at $k_z = \frac{1}{2}$ the phase change between adjacent unit cells results in a bonding orbital becoming an antibonding one during the transformation, causing an orbital crossing in $E(\vec{k}, q)$. a, b refer to antibonding and bonding character between adjacent atoms. The g, u labels are the conventional ones and refer to the inversion center at the midpoint of the unit cell in diagram (1). The unit cell is indicated in the first of the diagrams in this figure.

ics of the transformation depends on the orbital occupancy. For our "solid" of composition P_2^{4-} (isoelectronic with Cl_2), only the uppermost level at each point in \vec{k} space is unoccupied. As may readily be seen from Fig. 5(b), the energy changes with q associated with double-electron occupation of the lowest six orbitals will be small. The change in energy of each orbital is compensated by the change in energy of opposite sign associated with its partner. However, the occupied level which corresponds to $2\sigma_g^+$ in the molecular case has an unoccupied counterpart in this system, and a large, uncompensated increase in energy arises from this source as q increases from zero. At $k_z = \frac{1}{2}$, a point in \vec{k} space which possesses the full holohedral symmetry, a classic Woodward-Hoffmann HOMO-LUMO crossing is required by symmetry, with all the energetic repercussions noted previously. At adjacent lower-symmetry \vec{k} points (e.g., $k_z = \frac{3}{8}$) there is no crossing, the symmetry labels being only σ or π , but there is still a large energy barrier to the reaction, as would be expected from the continuity of the energy levels with \vec{k} . If we estimate the reaction barrier of process diagram (1) by averaging over the special \vec{k} points ($k_z = \frac{1}{16}, \frac{3}{16}, \frac{5}{16}$, and $\frac{7}{16}$, at $q = 0$ and $q = 0.5$, we obtain a reaction barrier of 3.9 eV, to be compared with an energy change of 2.2 eV at $k_z = 0$. (Note that the absolute values of these energies are probably meaningless, as the extended Hückel method is not expected to give accurate bond-dissociation energies, bond lengths, or force constants. However, the values do illustrate the effect of the symmetry-enforced crossings at the zone edge on the reaction barrier.)

It is obviously possible to modify the system so as to remove the crossings forced at $k_z = \frac{1}{2}$. Simply replacement of a homonuclear by a heteronuclear diatomic building block will allow the two crossing orbitals at $k_z = \frac{1}{2}$ to become of the same symmetry and "repel" in a similar fashion to that seen at points other than $k_z = 0$ or $\frac{1}{2}$ in the homonuclear case.

However, these avoided crossings will still give rise to a kinetic barrier to the process. The size of this barrier will be dependent on the efficiency of the orbital mixing, in turn related to how different the two atoms are in the building block.

This example clearly demonstrates that one might expect symmetry-imposed orbital crossings at certain points on the boundary of the Brillouin zone in transformations when bonds are broken within the unit cell and remade across unit-cell boundaries, and where a symmetry element bisects these linkages. Our two- and three-dimensional examples discussed below are considerably more complex, but at the simplest level many of the important features of the $E(\vec{k}, q)$ surfaces can be understood by analogy with this simple one-dimensional example.

VI. TWO-DIMENSIONAL POLYMERIZATION OF S_2N_2 TO $(SN)_x$

Solid-state polymerization is at present the most successful method for the production of large single crystals of a polymer, and hence there is considerable interest in the design of this type of polymorphic phase transition. In this section we investigate the polymerization of square planar molecules in a two-dimensional lattice, to give *cis* and *trans* polymer chains. A geometrical model which is applicable to the polymerization of S_2N_2 to $(SN)_x$ is discussed in the Appendix. The solid-state polymerization of S_2N_2 readily occurs at 0°C and leads to the *cis* polymer $(SN)_x$, which has been the subject of numerous experimental¹²⁻¹⁴ and theoretical studies^{7,15} because of its unusual metallic properties.

The reaction pathways studied for the formation of the two products are shown in Fig. 7. The route to the *cis* isomer involves the breaking and making of one bond per unit cell, and is simply related to the one-dimensional chain. However, there is no symmetry element bisecting the making or breaking bonds and so we do not expect to see symmetry-induced crossings on the $E(\vec{k}, q)$ surface. Similarly, the route for the formation of *trans* $(SN)_x$ involves the making and breaking of two bonds per unit cell, one along x and the other along the y direction. Here the only symmetry element (apart from the mirror in the plane of the molecule, giving σ and π symmetry types at all points in \vec{k} space), is a diagonal mirror,

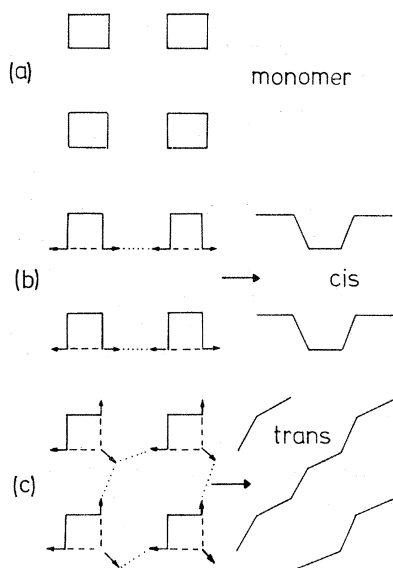
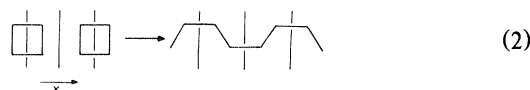


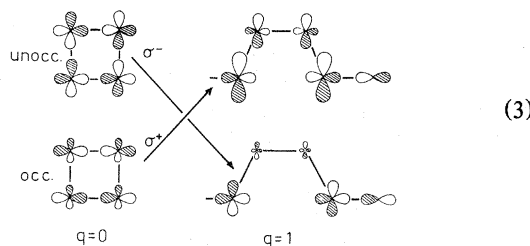
FIG. 7. Model reaction mechanisms for the polymerization of S_2N_2 to (b) *cis* $(SN)_x$ and (c) *trans* $(SN)_x$. Dashed lines; bonds to be broken. Dotted lines; bonds to be made. The idealized monomer structure is shown in (a). Each square represents an S_2N_2 molecule.

which does not bisect the making and breaking linkages and so does not provide a sufficient constraint on the orbital symmetry properties for crossings to be possible. Figures 8(a) and 8(b) show some slices through the $E(\vec{k}, q)$ surfaces for both transformations, which show avoided crossings at \vec{k} points where $k_x = \frac{1}{2}$ for the *cis* polymer and whenever either k_x or $k_y = \frac{1}{2}$ for the *trans* polymer. At $\vec{k} = (\frac{1}{2}, \frac{1}{2})$ for the *trans* polymer, the crossing is narrowly avoided and the $q = 0$ HOMO (σ -type orbital) actually crosses the $q = 0$ LUMO (a π -type orbital) along the distortion coordinate. We ascribe the larger reaction barrier in the *cis* case to the fact that two linkages per S_2N_2 molecule are stretched, to get to the intermediate, but only one in the *trans* case. Both routes are thus thermally allowed in the Woodward-Hoffmann sense (as we have already demonstrated by different methods for the *cis* isomer³). However, the question arises as to whether the reaction barriers arise from a close resemblance to a more symmetric system which does have crossings (i.e., is there here a barrier caused by approximate symmetry?).

We investigated this possibility by considering the same geometric problem but one in which all the atoms are identical. This introduces mirror planes bisecting the bonds which are broken and made to give the *cis* isomer, as shown in diagram (2).



As might be predicted from the discussion of the one-dimensional linear chain, there are now orbital crossings in our slices through the $E(\vec{k}, q)$ surface for $k_x = \frac{1}{2}$, as shown in Fig. 8(c). The effect of the reduction of symmetry between Figs. 8(b) and 8(c) is clear to see, and the diagrammatic representation of the orbitals involved in this crossing [diagram (3)] emphasizes the analogy with the linear chain. Thus the thermal polymerization of S_2N_2 to *cis* $(SN)_x$ is only "allowed" because there is no mirror plane bisecting the bonds in the real system. However, it is worth noting that the actual polymerization of S_2N_2 appears to involve a free radical intermediate.¹²



The reaction route postulated for the formation of

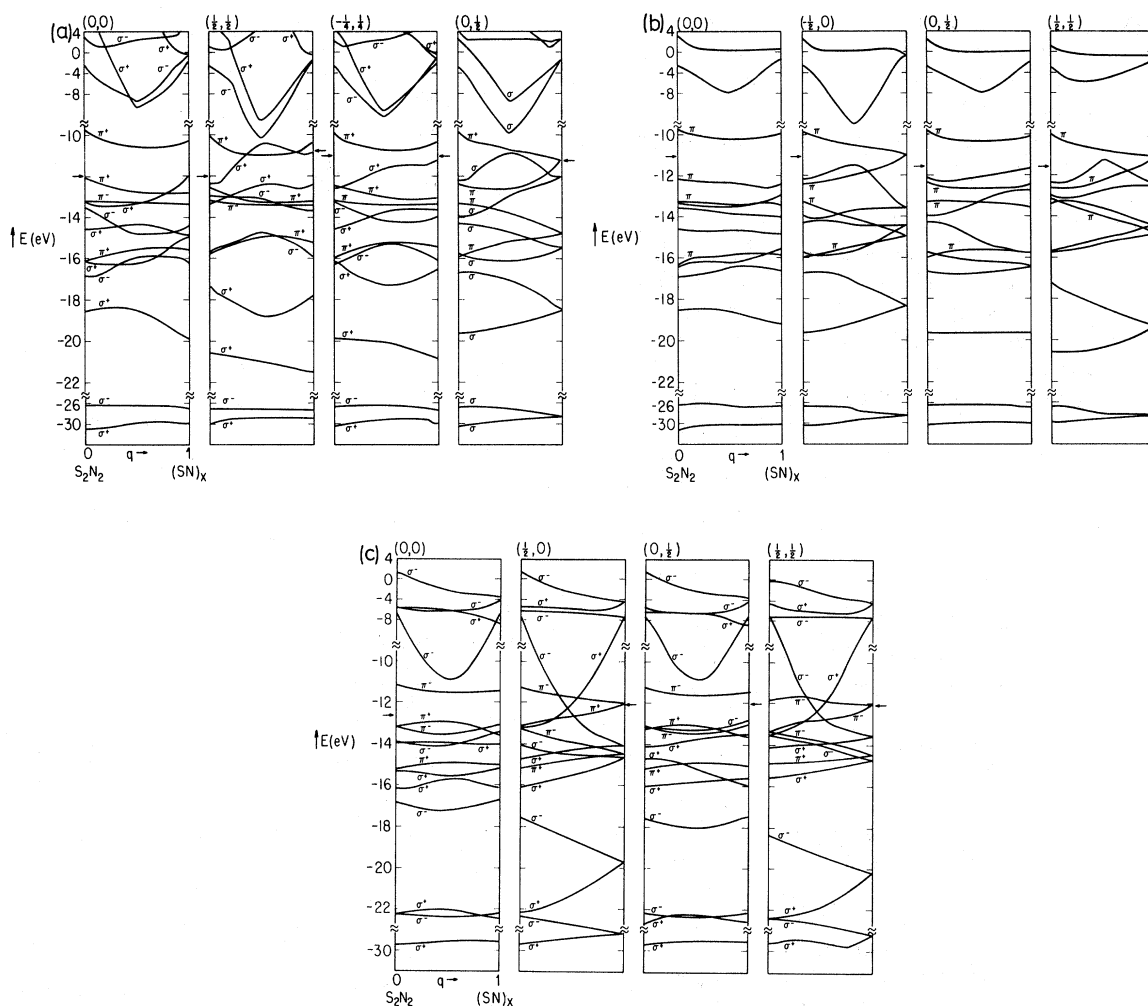


FIG. 8. Slices through $E(\vec{k}, q)$ for (a) formation of the *trans* $(\text{SN})_x$ polymer, (b) formation of the *cis* $(\text{SN})_x$ polymer, and (c) formation of *cis* $(\text{Ns})_x$ polymer where all the atoms of the system are made identical (Ns) as in diagram (2). Note that all orbitals stick together in pairs at $k_x = \frac{1}{2}$ for the *cis* polymer, since at this geometry there is a twofold screw axis along x (Herring's theorem). This accounts for the unusual metallic properties observed for *cis* $(\text{SN})_x$. Similarly, the *trans* polymer, with all bond lengths equal ($q = 1$) has extra symmetry which causes the orbitals to stick together in pairs at $k_x = \frac{1}{2}$ or equivalently $k_y = \frac{1}{2}$. The symmetry labels σ, π refer to symmetry or antisymmetry with respect to the plane containing the reacting molecules. The $+, -$ labels describe the parity with respect to reflection in the vertical mirror plane for the case of the *trans* isomer formed from S_2N_2 and the *cis* isomer formed from $(\text{Ns})_4$. Electrons fill the levels to the extent indicated by the arrows. Note the scale change at the top of the diagram. Note scale changes at top and bottom of diagram.

the *trans* polymer does not have any extra symmetry if all the atoms are of the same type. Coupled with our earlier comments, the fact that this *trans* $(\text{SN})_x$ has not been made cannot be attributed to a reaction coordinate with a *symmetry imposed* kinetic barrier. The formation of *trans* isomer is probably unfavorable because of a high reaction barrier for the polymerization process (*vide supra*) and because *trans* $(\text{SN})_x$ is thermodynamically less stable than the *cis* form.

VII. BLACK PHOSPHORUS TO ARSENIC TRANSFORMATION

The rhombohedral ($A7$) arsenic layer structure and the black phosphorus layer structure are found for some of the Group-V elements and IV/VI isoelectronic derivatives such as GeS and GeTe. One extremely useful geometrical and electronic way to view these structures is as distorted rocksalt arrangements,¹⁶ as we describe in detail elsewhere.¹⁷ Figure

9 shows how these two structures may be derived by breaking three mutually orthogonal linkages around each octahedrally coordinated rocksalt site. On squeezing black phosphorus, at 50 kbar a transformation occurs to the $A7$ structure.^{18,19} In this section we investigate theoretically how this transformation might proceed.

Geometrically we may divide the possibilities into two types, those where bonds are made and broken within the sheets of Fig. 9(a) and those where bonds are made between the sheets. In the latter category fall some interesting possibilities. We could remake all the linkages initially broken in the derivation from rocksalt, and then break a different set of linkages to produce the geometry of the product. Figure 9 shows the simplest such route where only some of these linkages are made and broken. We shall spend some time looking at $E(\vec{k}, q)$ surface for this process.

The unit cell for the intermediate ($0 < q < 1$) geometry is shown in Fig. 10(a). The structure belongs to the monoclinic space group, $P2/m$ (number 10). This symmorphic space group contains the essential symmetry elements $\{E|000\}$, $\{C_{2z}|000\}$, and $\{I|000\}$ in the usual Seitz nomenclature. At the points Γ , B , Y , Z , C , D , A , and E in the Brillouin zone [Fig. 10(b)] the group of \vec{k} is isomorphic with the point group C_{2h} with possible irreducible representations A_g, A_u, B_g, B_u . Here, as usual, A, B represent symmetric and antisymmetric behavior with respect to the C_2 operation and g and u corresponding behavior with respect to the inversion operation. The product $C_2 \times I$ leads to a mirror plane σ_{xy} . The lines Λ^x, V^x, W^x , and U^x have lower symmetry. Here the group of \vec{k} corresponds to the point group C_2 with possible irreducible representations A and B .

At $q = 0$, the black phosphorus structure the space group is number 53, $Pmna$ and at $q = 1$, the arsenic

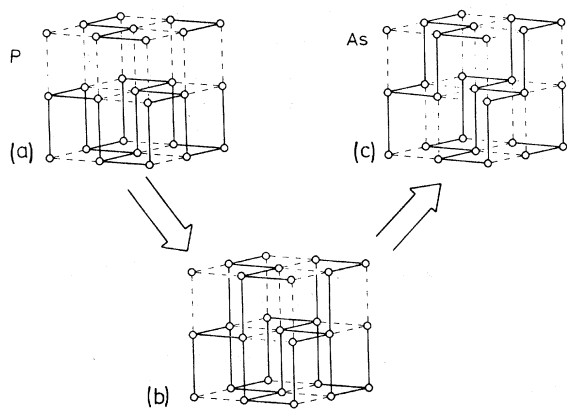


FIG. 9. Derivation of the arsenic (c) and black phosphorus (a) structures from rocksalt by bond breaking processes, and the simplest route for their interconversion by remaking some of these linkages (b).

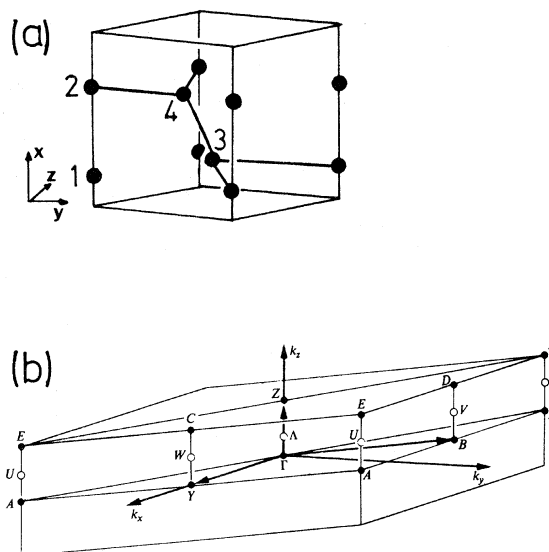


FIG. 10. (a) Unit cell for the monoclinic intermediate of the transformation depicted in Figs. 9 and 10. The separation of atoms 1 and 2 increases with q the reaction coordinate. (b) The Brillouin zone of (a) identifying the high-symmetry \vec{k} points: $\Gamma = (0, 0, 0)$, $B = (\frac{\pi}{2}, 0, 0)$,

$Y = (0, \frac{\pi}{2}, 0)$, $Z = (0, 0, \frac{\pi}{2})$, $C = (0, \frac{\pi}{2}, \frac{\pi}{2})$, $D = (\frac{\pi}{2}, 0, \frac{\pi}{2})$, $A = (\frac{\pi}{2}, \frac{\pi}{2}, 0)$, $(\frac{\pi}{2}, \frac{\pi}{2}, \frac{\pi}{2})$, or $(\frac{\pi}{2}, \frac{\pi}{2}, 0)$, $E = (\frac{\pi}{2}, \frac{\pi}{2}, \frac{\pi}{2})$, $(\frac{\pi}{2}, \frac{\pi}{2}, \frac{\pi}{2})$, or $(\frac{\pi}{2}, \frac{\pi}{2}, \frac{\pi}{2})$, $\Lambda^x(\Gamma Z)$, $V^x(BD)$, $W^x(YC)$, $U^x(AE)$.

structure, number 12, $C2/m$. The cell of Fig. 10 at either of these two q points is not the smallest that we could have chosen. The arsenic structure, for example, is usually referred to a two-atom rhombohedral cell. A symmetry analysis of the orbitals at, for example, $q = \frac{1}{8}$ and $\frac{7}{8}$, using the space group of the intermediate, is all that is required for demonstrating the existence of HOMO-LUMO crossings on the $E(\vec{k}, q)$ surface. However, the extra screw or glide symmetry elements in the space groups of the end points ($q = 0$ and $q = 1$) cause the orbitals to stick together in pairs at certain \vec{k} points on the zone surface, as described by Herring.^{10,11} This strong symmetry control of the orbital energy pattern of the arsenic and black phosphorus structures is very important in determining the form of the $E(\vec{k}, q)$ surface associated with their interconversion.

Figure 11 shows the correlation diagrams at several \vec{k} points for the transformation. Importantly, "HOMO-LUMO" crossings are only found for points on the $k_x = \frac{1}{2}$ surface of the Brillouin zone, and the behavior of the orbitals at these points is very similar to that seen for the linear chain, since bonds are made and broken along the x direction. The orbital descriptions are a little different since bonding is

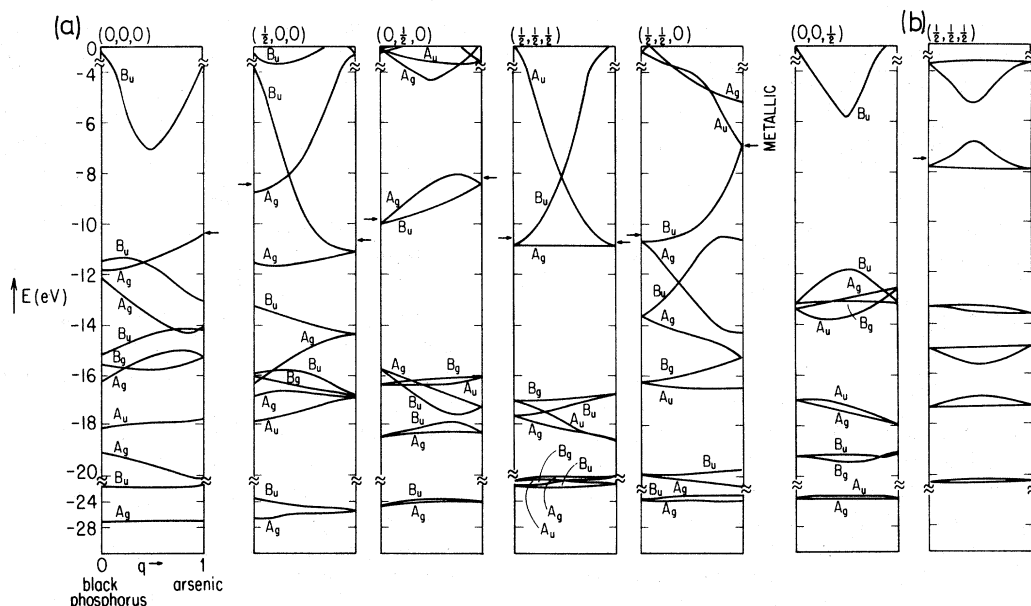


FIG. 11. (a) Slices through the $E(\vec{k}, q)$ surface for the black phosphorus ($q = 0$) to arsenic ($q = 1$) structural transformation for elemental phosphorus. (b) The $\vec{k} = (\frac{1}{2}, \frac{1}{2}, \frac{1}{2})$ slice through the $E(\vec{k}, q)$ surface for the same transformation (Fig. 9), for the derivative structure GeS, showing the avoided crossing. Symmetry labels are those for the C_{2h} point group, isomorphic with the group of \vec{k} for the high-symmetry \vec{k} points in the $P2/m$ space group.

maintained in the y and z directions. The postulated transformation mechanism is therefore represented by an $E(\vec{k}, q)$ surface with HOMO-LUMO crossings at certain points in \vec{k} space, and thus, according to our theory, cannot proceed martensitically.

The mechanism which we have studied is probably the simplest, least motion intersheet pathway for interconverting the black phosphorus and $A7$ structures. Naturally other mechanisms could be postulated, involving the making and breaking of many more bonds per unit cell. Alternatively, a sheet of the black phosphorus structure could be transformed into a sheet of the arsenic structure by the inversion of the local geometry (cf. ammonia) at half of the atomic centers, plus some "shuffling" rearrangements. However, if the inversion step is concerted, the intermediate for this pathway would have P-P linkages 7.5% shorter than those in the high pressure $A7$ form of phosphorus and hence such a mechanism is likely to have a high activation energy.

The black phosphorus to arsenic structural transformation has only been studied using polycrystalline aggregates in a diamond anvil cell. The transition occurs around 50-kbar pressure¹⁸ and is not readily reversible. The black phosphorus obtained after passing through the pressure cycle contained only crystallites. These observations suggest that the transformation proceeds by a nucleation and growth process, which is consistent with the conclusions of the study. It is hoped that sufficient information about this

structural transformation to distinguish between certain mechanisms may be obtained from studying a single crystal under pressure. It is perhaps worth noting that GeS, which crystallizes in an ordered variant of the black phosphorus structure, has been observed to transform under pressure to the rocksalt structure, and an $A7$ (arsenic) phase has not been reported. Phosphorus itself in the $A7$ structure, transforms to the rocksalt structure at higher pressures (111 ± 9 kbar).¹⁸ The lower symmetry in GeS prevents HOMO-LUMO crossings on the $E(\vec{k}, q)$ surface [Fig. 11(b)], though, as in the formation of cis (SN)_x, there is a reaction barrier due to the "intended" crossing. A fuller understanding of this type of structural transformation will require further experimental work on perhaps single crystals of GeS.

VIII. CONCLUSION

The present study is an attempt to interpret first- and second-order phase transitions in the solid state, in terms of underlying, fundamental orbital properties of the band structures of the initial, final, and intermediate geometries of the transforming phase. The most interesting idea to emerge from consideration of possible solid-state orbital correlation diagrams [$E(\vec{k}, q)$] is the suggestion that reaction mechanisms which involve the crossings of occupied and unoccupied orbitals on an $E(\vec{k}, q)$ surface cannot

proceed with approximate retention of translation symmetry. This hypothesis does require more strenuous testing and we are still searching for transformations which could be meaningfully examined using an $E(\vec{k}, q)$ surface and which would provide a stringent test of the theory. We have been unable to find, for example, a pair of reactions which, depending on the geometrical details of the two transformations, are predicted to be forbidden via one route but allowed via another in much the same way as the con- and disrotary ring closing reactions of 1–3 dienes.¹

The various systems studied in this work suggest that transformations which involve the breaking of bonds within the unit cell and the formation of bonds across unit-cell boundaries may often have crossings on an $E(\vec{k}, q)$ surface due to the phase differences between adjacent unit cells at certain points in \vec{k} space, provided that there are symmetry elements linking the moving atoms. There may still be a large reaction barrier if the symmetry is only approximate. Thus such reactions have a symmetry-imposed reaction barrier, and by our hypothesis, have to proceed via a nucleation and growth mechanism. This is a new explanation for the empirical observation that “bond breaking and remaking” transformations usually proceed by this mechanism, although the present state of this experimental area is one which has not been exhaustively studied.

ACKNOWLEDGMENTS

This research was supported by the National Science Foundation under Grant No. NSF DMR 8019741. We are grateful to S. Lee, T. J. McLarnan, and J. C. Jamieson for their help and interest and to M.-H. Whangbo for the use of his program.

APPENDIX

Details of models used for calculating $E(\vec{k}, q)$ surfaces.

(1) *NaCl in sodium chloride to cesium chloride structure.* Unit cell: Centered rhombohedron with NaCl distance kept constant at 2.814 Å.

Extended Hückel parameters		
Na $\zeta=0.733$	$H_{ss}=-5.1$ eV	$H_{pp}=-3.0$ eV
Cl $\zeta=2.033$	$H_{ss}=-30.0$ eV	$H_{pp}=-15.0$ eV

(2) *One-dimensional chain of P_2^{4-} molecules.* This system was chosen for the analogy with the bond reformation in the black phosphorus study. Unit cell length, $a=5.42$ Å. Bond length at $q=0$ and 1, $l=2.15$ Å.

Extended Hückel parameters		
P $\zeta=1.6$	$H_{ss}=-18.6$ eV	$H_{pp}=-14.0$ eV

(3) *Polymerization of $(SN)_x$.* Model as in Fig. 7, with $a=4.55$ Å and $l=1.65$ Å. This structural model was based on a proposal for a mechanism for the formation of the observed (*cis*) $(SN)_x$ from S_2N_2 put forward by Cohen *et al.*,¹² in which the polymerization occurs by a bond reformation process along the a axis of (S_2N_2) . Such a mechanism, combined with some rotation and translational shuffling transforms the $(0\bar{1}1)$ projection plane of S_2N_2 into the $(\bar{1}02)$ plane of $(SN)_x$.

Our model is a highly symmetrical idealization of the $(0\bar{1}1)$ plane of S_2N_2 , derived by

- (1) assuming S_2N_2 is orthorhombic (it is actually monoclinic with $\beta=106^\circ$),
- (2) assuming all SN bond lengths equal at $l=1.65$ Å (actual values 1.657 and 1.651 Å),
- (3) rotating alternate rows of molecules so that all molecules lie in the plane,
- (4) taking x axis through centers of molecules at 000 and 100 with $a=4.55$ Å (actual distance in S_2N_2 , 4.485 Å), and y axis 000 to $0\frac{1}{2}\frac{1}{2}$ with $b=a=4.55$ Å (in S_2N_2 distance is 4.627 Å).

Note that the separation between $(0\bar{1}1)$ planes is 3.44 Å, sufficiently long to justify our two-dimensional treatment. The model for forming *trans* $(SN)_x$ was the simplest we could devise for the formation of this hypothetical polymer from our two-dimensional model of S_2N_2 .

Extended Hückel parameters

N $\zeta=1.950$	$H_{ss}=-26.0$ eV	$H_{pp}=-13.4$ eV
S $\zeta=1.817$	$H_{ss}=-20.0$ eV	$H_{pp}=-13.3$ eV
Ns $\zeta=1.884$	$H_{ss}=-23.0$ eV	$H_{pp}=-13.4$ eV

The parameters for a mythical atom Ns were used for the study of Fig. 8(c) to replace those for both S and N, thus making all atoms identical.

(4) *Black phosphorus to arsenic structure.* The structure of the intermediate has space group $P2_1/m$, $a=5.42$ Å, $b=c=3.83252$ Å $=a/\sqrt{2}$, $\alpha=\beta=\gamma=90^\circ$, and atoms at the following positions: $\delta 0.89720 0 \bar{\delta} 0.1028 0$, $0.30140 0.6028 0.5$, $0.69860 0.39720 0.5$ where $\delta=0.3014+q$ ($0.1986-0.3014$). The black phosphorus ($q=0$) and arsenic structure ($q=1$) were taken from the slight idealization of the real structures, formed by deriving them from the rocksalt structure as described by Burdett and McLarnan.¹⁷ GeS was modeled by keeping all the interatomic distances for phosphorus and using the second row atoms Si and S.

Extended Hückel parameters

P $\zeta=1.6$	$H_{ss}=-18.6$ eV	$H_{pp}=-14.0$ eV
Ge $\zeta=1.383$	$H_{ss}=-17.3$ eV	$H_{pp}=-9.2$ eV
S $\zeta=1.817$	$H_{ss}=-20.0$ eV	$H_{pp}=-13.3$ eV

- *Present address: University Chemical Laboratories, Lensfield Road, Cambridge, CB2 1EW, United Kingdom.
- ¹R. B. Woodward and R. Hoffmann, *The Conservation of Orbital Symmetry* (Verlag Chemie GmbH, Weinheim, 1970).
- ²R. G. Pearson, *Symmetry Rules for Chemical Reactions* (Wiley, New York, 1976).
- ³J. K. Burdett, *J. Am. Chem. Soc.* **102**, 5458 (1980).
- ⁴A. H. Hever and G. L. Nord, in *Electron Microscopy in Mineralogy*, edited by H.-R. Wenk (Springer-Verlag, Berlin, 1976).
- ⁵J. W. Christian, *The Theory of Transformations in Metals and Alloys* (Pergamon, New York, 1965).
- ⁶L. Merrill, *J. Phys. Chem. Ref. Data* **6**, 1205 (1977).
- ⁷See, for example, M.-H. Whangbo, R. Hoffmann, and R. B. Woodward, *Proc. R. Soc. London, Ser. A* **366**, 23 (1979).
- ⁸S. W. Kennedy, *J. Solid State Chem.* **34**, 31 (1980).
- ⁹See for example, G. Herzberg, *Spectra of Diatomic Molecules* (Van Nostrand, New York, 1950).
- ¹⁰C. Herring, *Phys. Rev.* **52**, 361 (1937).
- ¹¹C. Herring, *Phys. Rev.* **52**, 365 (1937).
- ¹²M. J. Cohen, A. F. Garito, A. J. Heeger, A. G. MacDiarmid, C. M. Mikulski, M. S. Saran, and J. Kleppinger, *J. Am. Chem. Soc.* **98**, 3845 (1976).
- ¹³M. J. Cohen, C. K. Chiang, A. F. Garito, A. J. Heeger, C. M. MacDiarmid, and A. G. Mikulski, *Bull. Am. Phys. Soc.* **20**, 360 (1975).
- ¹⁴M. Boudelle, *Cryst. Struct. Comm.* **4**, 9 (1975).
- ¹⁵See H. Kamimura, A. M. Glazer, A. J. Grant, Y. Natsume, M. Schreiber, and A. D. Yoffe, *J. Phys. C* **9**, 291 (1976) and references therein.
- ¹⁶D. M. Adams, *Inorganic Solids* (Wiley, New York, 1974).
- ¹⁷J. K. Burdett and T. J. McLarnan, *J. Chem. Phys.* **75**, 5764 (1981).
- ¹⁸J. C. Jamieson, *Science* **139**, 1291 (1963).
- ¹⁹L. Cartz, S. R. Srinivasa, R. J. Riedner, J. D. Jorgensen, and T. G. Worlton, *J. Chem. Phys.* **71**, 1718 (1979).